BNL-223680-2022-JAAM

Unveiling the Degradation Mechanism of High-Temperature Superconductor $Bi_2Sr_2CaCu_2O_{8+\delta}$ in Water-Bearing Environments

Y. Huang, G. Gu

To be published in "ACS APPLIED MATERIALS & INTERFACES"

August 2022

Condensed Matter Physics and Materials Science Department

Brookhaven National Laboratory

U.S. Department of Energy

USDOE Office of Science (SC), Basic Energy Sciences (BES) (SC-22)

DISCLAIMER

Unveil the degradation mechanism of high-temperature superconductor $Bi_2Sr_2CaCu_2O_{8+\delta}$ in water-bearing environments

Yuan Huang[1,2#], Lei Zhang[2,3#], Xiao Cheng Zhou[4#], lei liao[2#], Feng Jin[2], Tao Dong[5], Lin Zhao[2], Qiuzhen Cheng[2], Qingming Zhang[2], Li Fen Wang[2], Nan Lin Wang[5], Ming Yue[3], Xuedong Bai[2], Ya Fei Li[4], Qiong Wu[3*], Hong-Jun Gao[2,7], Genda Gu[8], Yeliang Wang[1,6*], Xing-Jiang Zhou[2,7*]

[1]Advanced Research Institute of Multidisciplinary Science, Beijing Institute of Technology, Beijing, 100081, China

[2]Institute of Physics, Chinese Academy of Sciences, Beijing, 100190, China

[3]Faculty of Materials and Manufacturing, Key Laboratory of Advanced Functional Materials, Ministry of Education of China, Beijing University of Technology, Beijing, 100124, China

[4]Jiangsu Key Laboratory of New Power Batteries, Jiangsu Collaborative Innovation Centre of Biomedical Functional Materials, School of Chemistry and Materials Science, Nanjing Normal University, Nanjing 210023, China

[5]International Center for Quantum Materials, School of Physics, Peking University, Beijing, 100871, China

[6]School of Integrated Circuits and Electronics, MIIT Key Laboratory for Low-Dimensional Quantum Structure and Devices, Beijing Institute of Technology, Beijing, 100081, China

[7]University of Chinese Academy of Sciences, Beijing, 100049, China

[8]Condensed Matter Physics and Materials Science Department, Brookhaven National Lab, Upton, New York, 11973, USA

#These authors contributed equally to this work.
*Correspondence to: wuqiong0506@bjut.edu.cn; yeliang.wang@bit.edu.cn; xjzhou@iphy.ac.cn

Abstract

The physical properties of copper oxide high-temperature superconductors have been studied extensively, such as its band structure, and doping effects of $Bi_2Sr_2CaCu_2O_{8+\delta}$ (Bi-2212). However, some chemical-related properties of these superconductors are rarely reported, such as their stability in air. Here, we report experiments combined with ab initio calculations that address the effects of water in contact with Bi-2212. The evolution of Bi-2212 flake with exposure to water for different time intervals were tested and characterized by optical microscopy (OM), atomic force microscopy (AFM), Raman spectroscopy, transmission electron microscopy (TEM) and electrical measurements. The thickness of Bi-2212 flakes is gradually decreased in water, and some thin flakes can be completely etched away after a few days. The stability of Bi-2212 in other solvents is also evaluated, including alcohol, acetone, HCl and KOH. The morphology of Bi-2212 flakes is relatively stable in organic solvents. However, the flakes are etched relatively quick in HCl and KOH, especially in acidic environment. Our results imply that hydrogen ion is primarily responsible for the deterioration of their properties. Both TEM and calculation results demonstrate that the atoms in Bi-O plane is relatively stable when compared to the inner atoms in Sr-O, Ca-O and Cu-O planes. This work contributes towards understanding the chemical stability of Bi-2212 superconducting device in environmental medium, which is important for both fundamental studies and practical applications of copper oxide high-temperature superconductors.

1. Introduction

The chemical stability of low-dimensional materials is a key determinant factor for potential applications. In the family of two dimensional (2D) materials, graphene, h-BN and MoS_2 are relatively stable in air, while other layered materials have poor chemical stability. For example, black phosphorus, $MoTe_2$ and WTe_2 oxidizes easily in air[1-3], especially for monolayer and few layer samples. In the degradation process of 2D materials, defects and extra atoms are inevitably introduced, which can significantly disturb the observations of many important quantum phenomena. Therefore, unveiling the degradation mechanisms of 2D materials is not only helpful for understanding their chemical stability, but also important to find feasible protection strategies in applications.

Among many 2D materials, layered copper oxide materials stand out with their rich superconductivity behaviors. $Bi_2Sr_2CaCu_2O_{8+\delta}$ (Bi-2212) is one of the most well studied superconductors in layered copper oxide. The transition temperature (Tc) of Bi-2212 (~90 K) is above liquid nitrogen temperature (77 K), which makes it a viable material in many key superconductor applications, including cable for energy transmission[4], high field magnet[5], quantum computing[6-7] and weak signal detection devices[8]. The composition of the different elements in Bi-2212 crystal, especially the oxygen concentration, plays an important role for its superconductivity, which can significantly affect the critical transition temperature[9-10]. Many early studies on Bi-2212 focus mainly on the doping effects[11], such as Pb, La[12] , Ag[13] et al. While the physical properties of Bi-2212 and other copper-oxide superconductors have been well studied[6, 14-17], the chemical properties of this materials are rarely reported. As thickness decreases to monolayer and few layer, Bi-2212 becomes susceptible to degradation in air[15]. The instability of

Bi-2212 brings many difficulties for exploring the superconductive mechanism and applications, especially for monolayer or few layer samples. Among many gas molecules, water molecules are thought to have the dominant impact on the degradation of Bi-2212[18-19]. Therefore, it is important to understand the interaction mechanisms between water and superconducting oxides. In this study, we focus on one particular aspect that has not been addressed, the detailed degradation mechanism of Bi-2212 in air.

Here we discuss the results of a joint experimental and theoretical study with the goal of comprehensively addressing the interaction of Bi-2212 with H_2O and the impact on the electronic properties. The evolution of Bi-2212 flake with exposure to water was monitored by optical microscopy, atomic force microscopy (AFM) and Raman spectroscopy. By extending the immersion time of Bi-2212 crystal in water, the transition temperature clearly decreases and eventually, the superconductivity behavior completely disappears after 24 days in water. Transmission electron microscope (TEM) results demonstrate that the interlayer distance increases and the atoms become more random after water vapor treatment. More importantly, we find the Bi-O plane is much more stable than Cu-O, Bi-O and Ca-O plane. The Cu-O plane is prone to degradation in water, which directly affect the superconductivity behavior. Isotope labeling experiments using $H_2{}^{18}O$, combined with time-of-flight secondary ion mass spectrometry (TOF-SIMS) suggest that pristine 2D Bi-2212 can indeed react with water. DFT calculations reveal the detailed atomic processes of the interaction of 2D Bi-2212 with oxygen and water, showing that hydrogen ion is primarily responsible for the deterioration of their properties. Besides, the calculation results also indicate that Bi-O plane is more stable than other oxide planes in Bi-2212 crystal, which is consistent with the TEM results.

2. Results and Discussion

Bi-2212 flakes on SiO_2/Si support were prepared by a modified oxygen-plasma-enhanced exfoliation method[20], which helps to increase the yield and flake size. As shown in Figure 1, the morphology of Bi-2212 changes after exfoliation and taking out from water, which can be compared by optical images and AFM images. Figure 1a-c shows the schematics of the sample preparation and water treatment process. Figure 1d shows the optical microscopy image of freshly exfoliated Bi-2212 sample with monolayer and few layer flakes. It was subsequently immersed in DI water. After 48 h in DI water, the monolayer and few layer Bi-2212 areas are completely corroded (Figure 1e), while the outline of few layers zone can be still distinguished. To get the etching rate of Bi-2212 in water, the thickness of Bi-2212 were measured by atomic force microscopy (AFM) after taking out from water at different treatment times (Figure 1f-i). AFM images of a freshly exfoliated Bi-2212 flake (Fig. 1g) and the same flake after being submerged in DI water for 18 h (Fig. 1h) and 48 h (Fig. 1i) are also presented in Fig. 1. The thickness of one freshly exfoliated Bi-2212 flake in Fig. 1g is 20 nm. As the immersion time in water is extended, the thickness of the flake gradually decreases. The thickness of the flake decreased to 6 nm after 2 days (48 h) immersed in water. It can be observed that the surface of Bi-2212 become rough after taking out from water (Fig. 1i).

Other solvents are also tested for understanding the stability of Bi-2212, including HCl, NaOH, NaCl, acetone and ethanol (Figure S1-S3). The Bi-2212 flakes can be quickly etched in HCl, however, it's relatively stable in the organic solvents. Temperature has a significant effect on

degradation of Bi-2212. As shown in Fig. S4, monolayer and few layer Bi-2212 flakes can be quickly etched in hot water (temperature: 50 and 80 ℃) within a few hours. This results indicate that the degradation rate of Bi-2212 in water can be enhanced as temperature increase.

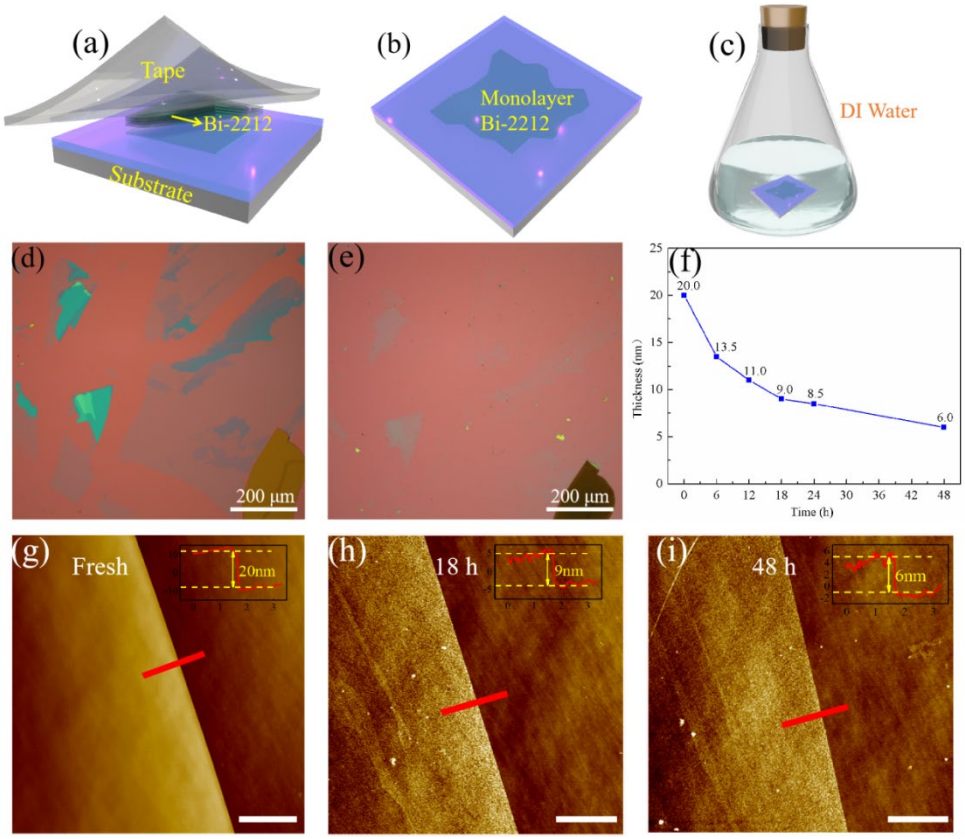

Fig. 1 Morphology change of exfoliated Bi-2212 flake on SiO_2/Si after immersion in DI water. (a-b) Schematic of the exfoliation and water treatment process. (c) Schematic of the setup used for the stability of Bi-2212 in DI water. (d) Optical image of a freshly exfoliated Bi-2212 flake. (e) Same flake after being immersed in DI water for 48 h. (f) The time dependency of thickness after put one Bi-2212 flake into water. (g-i) are the AFM images of a freshly exfoliated Bi-2212 flake and the same flake immersed in water for 18 h (h) and 48 h (i). The scale bar in (g-i) is 3 μm.

Raman scattering spectrum can provide lattice vibration-related information, which has been widely used for studying structural changes, strain, defects, and layer number in 2D materials. Here, we also use Raman spectroscopy to understand the lattice changes of Bi-2212 after water treatment. Before submerging Bi-2212 into water, three sharp Raman peaks can be observed at around 409, 463 and 627 cm^{-1}, which are assigned to the vibration of O(Cu) atoms in the Cu-O planes, the vibration of O(Bi) atoms in the Bi-O planes and the vibration of O(Sr) atoms in the Sr-O planes, respectively[21-23]. The peaks located at ~310 and 520 cm^{-1} originate from the Si basement[5,6]. After immersing the flake in water for 24 h, the spectra show two significant changes. Firstly, the phonon peak (409 cm^{-1}) due to the vibration of O(Cu) atoms almost disappears. Secondly, the phonon peaks at 463 cm^{-1} and 627 cm^{-1} due to the vibration of O(Cu) and O(Sr) atoms exhibits a substantial softening. These two distinct differences suggest that the Cu-O layers are more easily damaged in water. Moreover, the softening of the vibration of O(Bi) and O(Sr)

atoms suggests the Bi-O bonds and the Sr-O bonds also weakens after degradation of Cu-O layer. The conclusion extracted from Raman spectra changes is consistent with the TEM and calculation results presented below, which all suggest that the Cu-O layer is more sensitive to water.

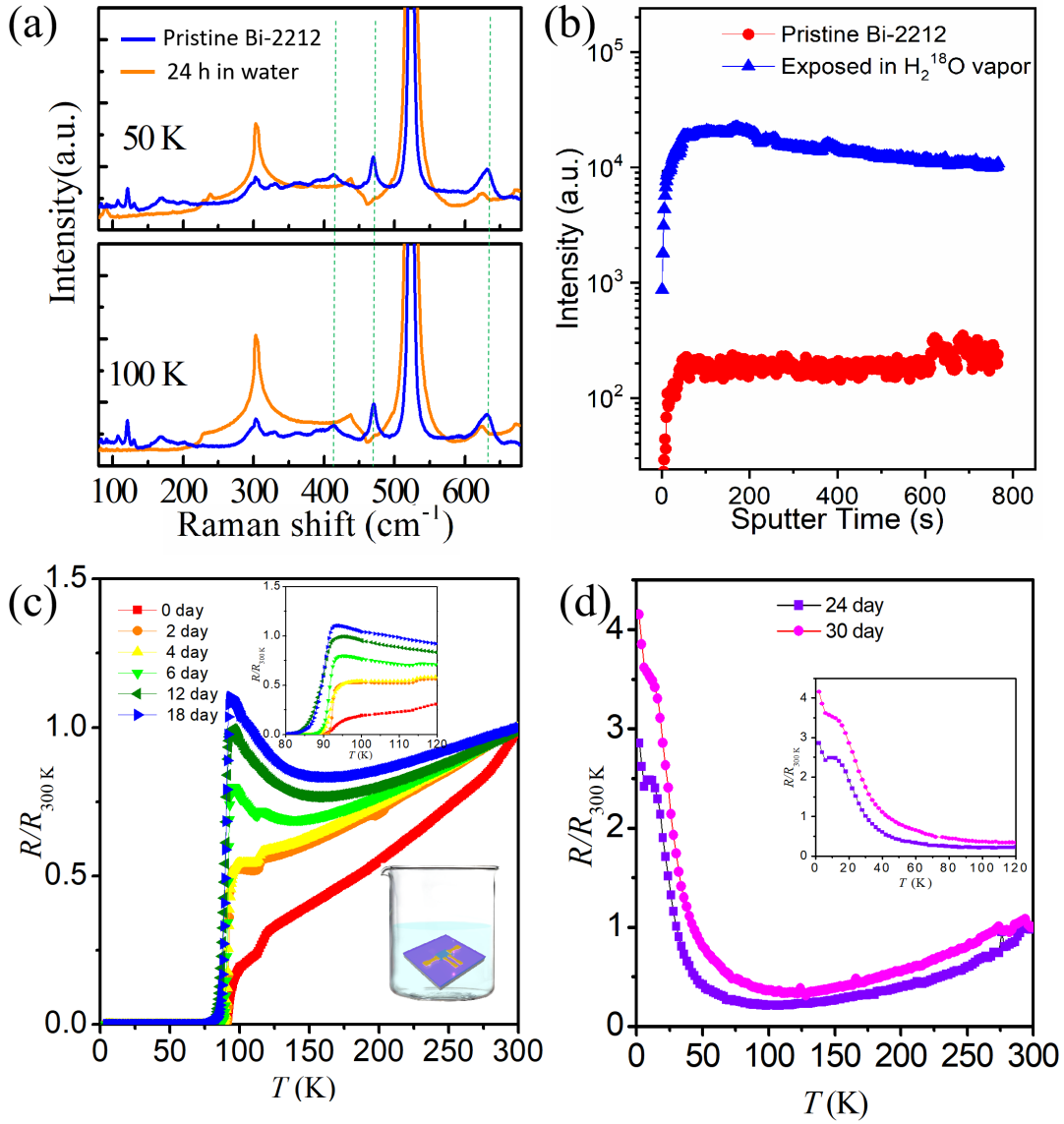

Fig. 2 Raman spectra, TOF-SIMS and transport measurements of Bi-2212 before and after immersion in water. (a) Raman spectra of Bi-2212 before and after reaction with water, which were measured at 50 K and 100 K. (b) TOF-SIMS results of ^{18}O intensity in pristine Bi-2212 (red curve) and the Bi-2212 crystal exposed in $H_2{}^{18}O$ vapor (blue curve). (c) Temperature-dependent resistance (R-T curves) of a freshly exfoliated Bi-2212 crystal and after immersion in water. The sample was taken out from water after 2, 4, 6, 12 and 18 days. The insets are the schematic image of the Bi-2212 device in water and the R-T curves in the range of 80 K to 120 K. (d) R-T curves of the Bi-2212 device after immersion in water for 24 and 30 days. The inset is the same curves from 0 K to 120 K range.

Isotope labeling experiment using $H_2{}^{18}O$ was carried out to further probe the interactions of Bi-2212 with water. To address this, we performed a precise chemical composition analysis of the Bi-2212 crystal by using Time-of-flight secondary ion mass spectrometry (TOF-SIMS). The

chemical compositions of Bi-2212 crystal before and after 24 hours exposure in water can be directly compared through the intensity curves of ^{18}O, as shown in Fig. 2b. On the general ion depth profile, the intensity of the ion signals ($^{18}O^-$) are plotted versus Cs^+ ion sputtering time. Ion's intensity is reported in logarithm scale. Intensity changes with the sputtering time on the profile reflect in-depth concentration variations [24]. As can be seen in Fig. 2b, the intensity of ^{18}O in fresh-cleaved Bi-2212 is around 200. However, this value increase to 20000 in the Bi-2212 crystal exposed in ^{18}O-labeled water, which increased about 100 times than the fresh Bi-2212. This result unambiguously confirms that Bi-2212 crystal has reacted with water.

Water is considered to be the main reason for the deterioration of Bi-2212 [25]. In order to study the effect of water on the superconductivity, we measured the transport of Bi-2212 crystal in contact with water for different times. Considering monolayer and few layer Bi-2212 degrade quickly in water, we choose bulk crystal to track electrical transport changes because it degrades slowly in water. For newly cleaved Bi-2212 crystal, its resistance changes dramatically with temperature, and the superconducting transition temperature (Tc) is 93.4 K (Fig. 2c). When Bi-2212 was in contact with water for two days, its superconducting transition temperature decreased only slightly to 92.1 K. After 6 days in water, the resistance continued to decrease linearly as a function of temperature, from 300 K to 150 K. However, the resistance starts to increase as temperature decrease from 150 K to 95 K. This indicates that part of the crystal is changing from metallic to partially insulating because of the oxide layers changes in water. With the extension of reaction time in water, the superconducting transition temperature decreases continuously, and the low-temperature resistance increases. After 24 and 30 days immersed in water, the superconductivity disappear, as shown in Fig. 2d.

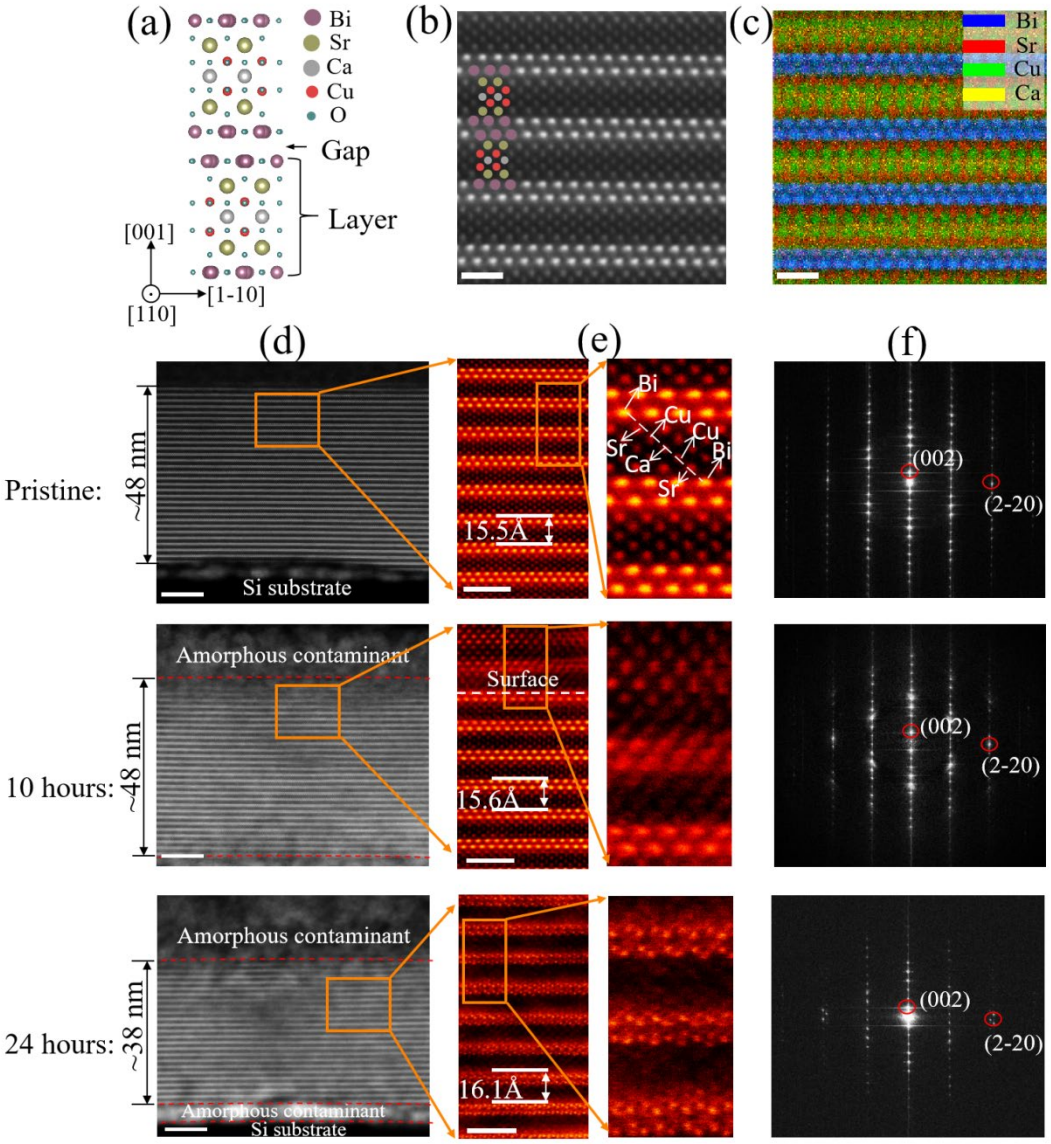

Figure. 3 Atomic resolution electron microscopy images of Bi-2212. (a) Atomic structure model of Bi-2212 along the [110] crystallography direction. (b) HAADF-STEM image of a Bi-2212 thin film viewed in cross section along the [110] zone axis, Scale bar: 1 nm. (c) The EDXS elemental map of Bi-2212 showing the cationic distribution, Scale bar: 1 nm. (d) Sequential HAADF images of a Bi-2212 thin film under water exposure, the view direction is along [110] crystallography zone-axis, scale bar: 10 nm. (e) High-resolution color-coded HAADF images of typical regions as marked by squares in (d), scale bar: 2 nm. The right part is zoom-in image of the left ones. (f) Corresponding FFT of images in 3e showing the structural evolution.

Figure 3a shows atomic structure of Bi-2212, each unit cell contains two layers separated by van der Waals gaps. Figure 3b shows a high-angle annular dark-field STEM (HAADF-STEM) image in [110] zone axis. This Z-contrast image (Z is the atomic number) presents the exact atomic stacking (Bi-Sr-Cu-Ca-Cu-Sr-Bi) of the Bi-2212 crystal structure, the corresponding atomic arrangements is schematically depicted on the left side of HAADF image. In figure 3c, atomically resolved STEM-EDX elemental map shows the cation distribution, which matches well with the crystal structure. By comparing the HAADF-STEM images, we find that the thickness of

the Bi-2212 thin film decreased after water processing (figure 3d). In the pristine state, the thickness of Bi-2212 thin film is ~48 nm. After 10 hours, the thickness remains almost the same. After 24 hours, however, the thickness decreased to ~38 nm. At the same time, the crystalline quality decreases and the lattice is distorted after water processing, as shown in figure 3e. In the pristine state, the HAADF image shows clear and uniform atomic arrangements, indicating high crystal quality, and the interlayer spacing is consistent with the theoretical value (15.596 Å). After 10 hours, most regions show the same structure as before, and the interlayer spacing slightly increases. On the surface regions, however, the contrast becomes darker, and the atomic arrangements are different when compared to the interior regions, where each atomic stacking shows uniform contrast rather than alternate contrast. The HAADF image contrast is based on atomic number and thickness (in the view direction), it can be inferred that the surface started to decrease in thickness and the elements diffuse to form different atomic arrangements. After 24 hours, the atomic arrangement become indistinct and disordered, that is, the Bi-O layers contain several split atom columns rather than single atom column and the other element layers become almost indistinguishable. This difference indicates that the Sr-O, Cu-O and Ca-O layers are more sensitive than Bi-O layer when interacting with water. The interlayer spacing is 16.1 Å, an increase of 3% compared to that of the pristine state. In figure 3f, the corresponding FFT images shows that the sharp diffraction spots in the pristine state become dispersive, and even split after water processing. Both STEM images and the corresponding FFT indicate poor crystal quality and lattice distortion after water treatment.

In previous studies, a few teams tried to unveil the interaction mechanism between copper oxide and water, but the detailed reaction processes have not been well understood. At room temperature, quick redox reactions with water can deteriorate the superconductivity of bulk cuprate superconductors by producing non-superconducting phases[26]. Rosamilia et al. showed the reaction[27]: $Cu^{+3} + 1/2H_2O \rightarrow H^+ + 1/4O_2 + Cu^{+2}$ (1). Non superconducting Bi_2CuO_4, $SrCO_3$, $CaCO_3$, and CuO were discovered as the resultant end products of the Bi-2212 water reaction[28]. It was also observed that partial loss of oxygen in the top-most layer of Bi-2212 crystal can also decrease the superconductivity[29-30]. However, the bare Bi-2212, when exfoliated in air to 2D atomic layer, is entirely insulating even in oxygen annealed atomosphere[31-32].

In order to provide insight into the surface changes of 2D Bi-2212 at the atomic level, theoretical investigations were carried out based on density functional theory (DFT) calculations. The interaction of Bi-2212 with H_2O and H_3O^+ are firstly considered. Here we use the structure of Bi-2212(001) film with an oxygen vacancy on the surface for calculation as vacancies are unavoidable during the growth process. The H_2O molecule is firstly physiosorbed on the surface as shown in Figure S5, where the chemisorption and dissociation of H_2O are investigated. At close to the surface, H_2O dissociates to form one hydrogen bonding with Bi atom and one OH^- group bonding with another Bi atom. The adsorption energy is about -0.04 eV, indicating the weak interaction between Bi-2212(001) film and H_2O. In addition, we also took a close look at the degradation process of Bi-2212(001) surface in coexistence with H_3O^+. Under this condition, hydrogen ion interacts strongly with the surface. The hydrogen atom is connected to the oxygen atom with energy release of 0.59 eV and forms a hydroxyl group, which is conductive to the subsequent reaction. To model the next step of degradation, we placed another H_3O^+ onto the

surface as shown in Figure 4. The hydrogen atom binds with the hydroxyl group and forms a H_2O molecule. At the same time, the Bi-O and Sr-O bond lengths are significantly enlarged, indicating the desorption of H_2O from the surface and the degradation of Bi-2212 crystal. The calculation results show that hydrogen ions are primarily responsible for the degradation of 2D Bi-2212, in agreement with the experimental results.

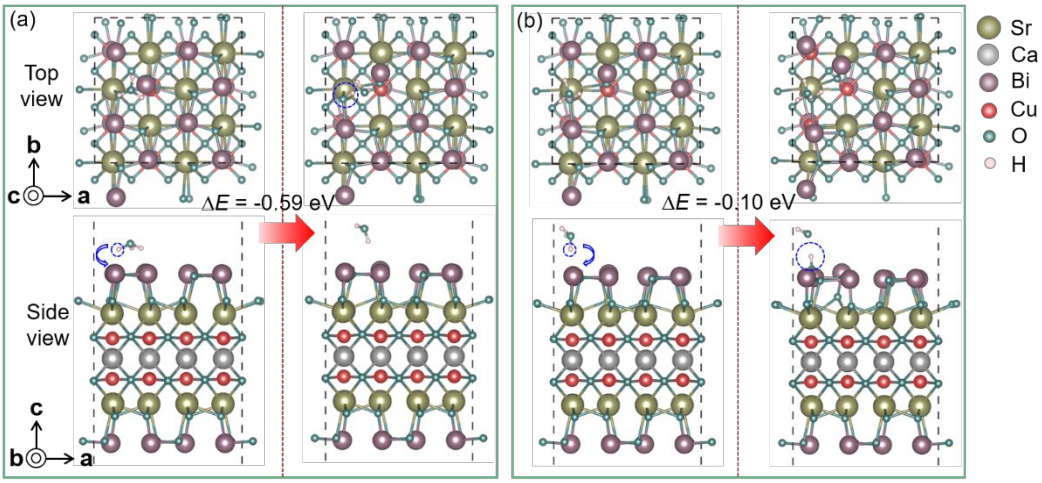

Figure 4. Hydrogen adsorption on Bi-2212(001) surface. (a) Initial and final atomic structures of the first H adsorption on the surface and the formation of OH group. (b) Initial and final atomic structures of the second H adsorption on the surface and the desorption of H_2O. The reaction process can be stated as: Bi-2212(001) + H_3O^+ → Bi-2212(H, H_2O).

To understand the effects of water on the Sr-O, Cu-O and Ca-O layers, we further investigate the interaction of these layers with the H_2O molecule at atomic level. Here we choose the Bi-2212(010) surface with Sr, Cu, and Ca atoms exposed on the surface to model the inner oxide layers. As illustrated in Figure 5, H_2O tends to chemisorb and dissociate at the Sr, Cu, and Ca sites on Bi-2212(010) surface with energy release of -3.07, -3.08, and -3.12 eV, respectively, which is higher than that of H_2O dissociation on Bi-2212(001) surface. These highly exothermic processes imply that the Sr-O, Cu-O and Ca-O layers react more strongly with H_2O than the Bi-O layer. As shown in the TEM results in Fig. 3e, the Sr-O, Cu-O and Ca-O layers are more easily destroyed than Bi-O layer when Bi-2212 is placed in direct contact with water.

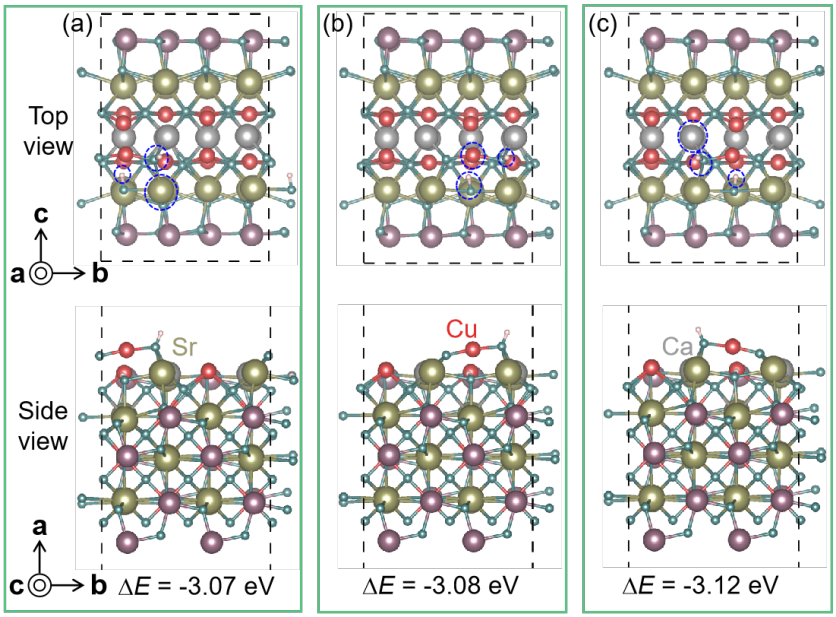

Figure 5. Adsorption and dissociation of H_2O on Bi-2212(010) surface. Atomic structures of chemisorbed and dissociated H_2O on the surface at the (a) Sr, (b) Cu, and (c) Ca sites.

Although past research have concluded that Bi-2212 is not stable in air and may react with water, the mechanism where this process occurs is still not well understood. In this study, we unveil the reaction mechanism of Bi-2212 with water in detail for the first time. Both experimental and calculation results demonstrate that the Bi-O layer is hydrophobic and relatively stable in water-bearing environment. However, the other oxide layers all show hydrophilic and high chemisorb energy, which tend to react with water. It is well known from studies of the past century that the Cu-O layer in copper-oxide-based materials determines the formation of the cooper pair and directly contribute towards its superconductivity. Once the oxygen atom concentration changes or the lattice structure destroyed, the superconductivity in copper-oxide-based superconductors will be severely affected. After this mechanism is clarified, the electrical transport behaviors of Bi-2212 in Fig. 2c-d can be easily understood. The Cu-O layer and neighboring oxide layers are easily changed in water environment, and as a result, the resistivity will increase before entering into superconductivity state, and superconductive transition temperature will decrease. In this stage, the cooper pair can still survive as Cu-O layers are not completely destroyed. After reaching a certain threshold, the superconductivity in Bi-2212 crystal will disappear as the cooper pair formation becomes suppressed on Cu-O layers.

3. Conclusion and perspective

In summary, the reaction mechanism of water molecule and Bi-2212 crystal is unveiled by combining experimental and calculation results. The Raman spectra results indicate that the Cu-O layers are more easily damaged in water. By using $H_2{}^{18}O$ as isotope labeling matter, the reaction mechanism between Bi-2212 and water can be unambiguously confirmed. Both TEM and calculation results demonstrate that the Bi-O surface is hydrophobic and is more stable than other oxide layers in Bi-2212 crystal. Our work not only clarifies the reaction process of water and

Bi-2212, but also bring inspiration for tuning the disorder in Bi-2212 crystal by water, which is important for understanding the origin mechanism of its superconductivity. In recent years, the relationships between Mott insulator state, strange metal state and superconductivity attracted much attention. Using water treatment for Bi-2212 may provide a simple and controllable way to achieve Mott insulator and strange metal states.

4. Method

Sample Preparation. The few-layer Bi-2212 was prepared using poly dimethylsiloxane (PDMS) stamp-assisted mechanical exfoliation method. Firstly, transfer the sample to PDMS and tear it 2-3 times to make the sheet thinner. Then, PDMS with Bi-2212 was pasted on the surface of 300 nm SiO_2/Si substrate. All the substrates were cleaned by oxygen plasma to remove organic residues before contact with Bi-2212, which improved the yield. Before stripping, the substrate and Bi-2212/PDMS were placed on a laboratory hot plate, annealed at 80 ℃ for 1 minute, and gentle pressure were applied to establish a good contact area between Bi-2212 and SiO_2 surface. Peeling off the PDMS removes the major portion of the crystal, leaving one or few large-area monolayer flakes on the SiO_2 surface. Limited only by the size of available bulk crystals, these monolayer flakes are usually macroscopic in size.

Material Characterization. Optical microscopy (Olympus BX53M with a CCD camera) was used to examine the dimensions and uniformity of the exfoliated 2D crystals. The morphology and thickness were investigated by atomic force microscopy (AFM, Bruker Multimode 8). AFM imaging was performed in ambient air at room temperature. The Raman measurements were performed with a backscattering configuration using a commercial Raman system (JY Horiba HR Evolution) and a helium-neon laser (λ = 632.8 nm). The laser beam was focused on the samples by an objective with beam diameter of about 2 μm. The laser power was kept at a level of 0.5 mW to avoid overheating. HAADF images for sample characterization were obtained using an aberration corrected JEOL Grand ARM 300 CFEG at 300 kV. The spot size was 8c, and the collection angles ranged from 54 to 220 mrad. The atomically resolved energy-dispersive X-ray spectroscopy (EDXS) maps were also recorded to determine cationic distribution.

Computational Method. All the DFT computations were performed via Vienna ab initio simulation package (VASP)[33]. The exchange correlation was described by Perdew-Burke-Ernzerhof (PBE) functional [34] and based on the generalized gradient approximation (GGA) method. And the ion-electron interaction was described with the projector-augmented plane-wave (PAW) method[35-36]. The energy cutoff for the plane-wave basis was set to 500 eV for all the computations. The *k*-space sampling was set as 4 × 4 × 1 for the Bi-2212 supercell, and the system were fully optimized until the convergence threshold energy and force are less than 1×10^{-5} eV and 0.01 eV/Å, respectively. A vacuum region of more than 15 Å was used to avoid the interaction between periodic surfaces. The adsorption on the surface was determined by allowing the top three layers together with the adsorbate to relax freely while the other bottom layers were fixed.

Acknowledgments

This work is supported by the National Key Research and Development Program of China (Grant No. 2019YFA0308000, 2021YFA1401800, 2018YFA0305800), the National Natural Science Foundation of China (Grant No. 62022089, 11874405, 11888101), Chongqing Outstanding Youth Fund (Grant No. 2021ZX0400005), the Strategic Priority Research Program (B) of the Chinese Academy of Sciences (Grant No. XDB33000000), and Natural Science Foundation of Jiangsu Higher Education Institutions of China (21KJB150028). The authors thank Dr. Norman N. Shi for helpful discussions.

Reference

1. Huang, Y.; Qiao, J.; He, K.; Bliznakov, S.; Sutter, E.; Chen, X.; Luo, D.; Meng, F.; Su, D.; Decker, J.; Ji, W.; Ruoff, R. S.; Sutter, P., Interaction of Black Phosphorus with Oxygen and Water. *Chemistry of Materials* **2016,** *28* (22), 8330-8339.

2. Zhu, H.; Wang, Q.; Cheng, L.; Addou, R.; Kim, J.; Kim, M. J.; Wallace, R. M., Defects and surface structural stability of MoTe2 under vacuum annealing. *Acs Nano 11*, 11005-11014.

3. Ye, F.; Lee, J.; Hu, J.; Mao, Z.; Wei, J.; Feng, P. X., Environmental Instability and Degradation of Single- and Few-Layer WTe2 Nanosheets in Ambient Conditions. *Small* **2016,** *12* (42), 5802-5808.

4. Bjoerstad, R.; Scheuerlein, C.; Rikel, M. O.; Ballarino, A.; Bottura, L.; Jiang, J.; Matras, M.; Sugano, M.; Hudspeth, J.; Di Michiel, M., Strain induced irreversible critical current degradation in highly dense Bi-2212 round wire. *Superconductor Science & Technology* **2015,** *28* (6).

5. Miao, H.; Marken, K. R.; Meinesz, M.; Czabaj, B.; Hong, S., Development of round multifilament Bi-2212/Ag wires for high field magnet applications. *Ieee Transactions on Applied Superconductivity* **2005,** *15* (2), 2554-2557.

6. Chen, S. D.; Hashimoto, M.; He, Y.; Song, D.; Xu, K. J.; He, J. F.; Devereaux, T. P.; Eisaki, H.; Lu, D. H.; Zaanen, J.; Shen, Z. X., Incoherent strange metal sharply bounded by a critical doping in Bi-2212. *Science* **2019,** *366* (6469), 1099-1102.

7. Kundu, A. K.; Wu, Z. B.; Drozdov, I.; Gu, G.; Valla, T., Origin of Suppression of Proximity-Induced Superconductivity in Bi/Bi2Sr2CaCu2O 8+ δ Heterostructures. *Advanced Quantum Technologies* **2020,** *3* (9), 2000038.

8. Liu, G. Y.; Bao, X. Z.; Dong, W. K.; Wei, Q.; Mu, H. R.; Zhu, W. G.; Wang, B. Z.; Li, J. D.; Shabbir, B.; Huang, Y.; Xing, G. C.; Yu, J. H.; Gao, P.; Shao, H. Y.; Li, X. P.; Bao, Q. L., Two-Dimensional Bi2Sr2CaCu2O8+delta Nanosheets for Ultrafast Photonics and Optoelectronics. *Acs Nano* **2021,** *15* (5), 8919-8929.

9. Miyakawa, N.; Guptasarma, P.; Zasadzinski, J. F.; Hinks, D. G.; Gray, K. E., Strong dependence of the superconducting gap on oxygen doping from tunneling measurements on Bi2Sr2CaCu2O8-delta. *Physical Review Letters* **1998,** *80* (1), 157-160.

10. Genoud, J. Y.; Triscone, G.; Junod, A.; Tsukamoto, T.; Muller, J., Reversible Magnetization as a Function of the Oxygen Concentration in Bi-2212 Superconducting Ceramics. *Physica C-Superconductivity and Its Applications* **1995,** *242* (1-2), 143-154.

11. He, Y.; Hashimoto, M.; Song, D.; Chen, S. D.; He, J.; Vishik, I. M.; Moritz, B.; Lee, D. H.; Nagaosa, N.; Zaanen, J.; Devereaux, T. P.; Yoshida, Y.; Eisaki, H.; Lu, D. H.; Shen, Z. X., Rapid change of superconductivity and electron-phonon coupling through critical doping in Bi-2212. *Science* **2018,** *362* (6410), 62-+.

12. Jin, H.; Kötzler, J., Effect of La-doping on growth and superconductivity of Bi-2212 crystals. *Physica C: Superconductivity* **1999,** *325* (3-4), 153-158.
13. Sotelo, A.; Madre, M.; Diez, J.; Rasekh, S.; Angurel, L.; Martinez, E., The influence of Pb and Ag doping on the Jc (H, T) dependence and the mechanical properties of Bi-2212 textured rods. *Superconductor Science and Technology* **2009,** *22* (3), 034012.
14. Fujita, K.; Noda, T.; Kojima, K. M.; Eisaki, H.; Uchida, S., Effect of disorder outside the CuO2 planes on T-c of copper oxide superconductors. *Physical Review Letters* **2005,** *95* (9).
15. Yu, Y. J.; Ma, L. G.; Cai, P.; Zhong, R. D.; Ye, C.; Shen, J.; Gu, G. D.; Chen, X. H.; Zhang, Y. B., High-temperature superconductivity in monolayer Bi2Sr2CaCu2O8+delta. *Nature* **2019,** *575* (7781), 156-+.
16. Zhang, Y. X.; Hu, C.; Hu, Y.; Zhao, L.; Ding, Y.; Sun, X.; Liang, A. J.; Zhang, Y.; He, S. L.; Liu, D. F.; Yu, L.; Liu, G. D.; Dong, X. L.; Gu, G. D.; Chen, C. T.; Xu, Z. Y.; Zhou, X. J., In situ carrier tuning in high temperature superconductor Bi2Sr2CaCu2O8+delta by potassium deposition. *Science Bulletin* **2016,** *61* (13), 1037-1043.
17. Ai, P.; Gao, Q.; Liu, J.; Zhang, Y. X.; Li, C.; Huang, J. W.; Song, C. Y.; Yan, H. T.; Zhao, L.; Liu, G. D.; Gu, G. D.; Zhang, F. F.; Yang, F.; Peng, Q. J.; Xu, Z. Y.; Zhou, X. J., Distinct Superconducting Gap on Two Bilayer-Split Fermi Surface Sheets in Bi2Sr2CaCu2O8+delta Superconductor. *Chinese Physics Letters* **2019,** *36* (6).
18. Jin, S. G.; Zhu, Z. Z.; Liu, L. M.; Huang, Y. L., Water Reactions of Superconducting Bi2sr2cacu2o8 Phase at 0-Degrees-C and Ambient-Temperature. *Solid State Communications* **1990,** *74* (10), 1087-1090.
19. Lee, D.; Condrate, R. A.; Taylor, J. A., The environmental degradation mechanism and protective organic thin film coatings on a high-temperature bismuth-cuprate superconductor. *Physica C* **2001,** *350* (1-2), 1-16.
20. Huang, Y.; Pan, Y. H.; Yang, R.; Bao, L. H.; Meng, L.; Luo, H. L.; Cai, Y. Q.; Liu, G. D.; Zhao, W. J.; Zhou, Z.; Wu, L. M.; Zhu, Z. L.; Huang, M.; Liu, L. W.; Liu, L.; Cheng, P.; Wu, K. H.; Tian, S. B.; Gu, C. Z.; Shi, Y. G.; Guo, Y. F.; Cheng, Z. G.; Hu, J. P.; Zhao, L.; Yang, G. H.; Sutter, E.; Sutter, P.; Wang, Y. L.; Ji, W.; Zhou, X. J.; Gao, H. J., Universal mechanical exfoliation of large-area 2D crystals (vol 11, 2453, 2020). *Nat. Commun.* **2020,** *11* (1), 1.
21. Kakihana, M.; Osada, M.; Kall, M.; Borjesson, L.; Mazaki, H.; Yasuoka, H.; Yashima, M.; Yoshimura, M., Raman-active phonons in Bi2Sr2Ca1-xYxCu2O8+d (x=0-1): Effects of hole filling and internal pressure induced by Y doping for Ca, and implications for phonon assignments. *Physical Review B* **1996,** *53* (17), 11796-11806.
22. Pantoja, A. E.; Pooke, D. M.; Trodahl, H. J.; Irwin, J. C., Oxygen-isotope effect on the high-frequency Raman phonons in Bi2Sr2CaCu2O8+delta. *Physical Review B* **1998,** *58* (9), 5219-5221.
23. Cooper, S. L.; Klein, M. V.; Pazol, B. G.; Rice, J. P.; Ginsberg, D. M., Raman-Scattering from Superconducting Gap Excitations in Single-Crystal Yba2cu3o7-Delta. *Physical Review B* **1988,** *37* (10), 5920-5923.
24. Cornette, P.; Zanna, S.; Seyeux, A.; Costa, D.; Marcus, P., The native oxide film on a model aluminium-copper alloy studied by XPS and ToF-SIMS. *Corrosion Sci.* **2020,** *174*, 8.
25. Liu, Y.; Chen, L.; Wang, M.; Zhang, X.; Li, X.; Sun, Y.; Jiang, D.; Hu, T., Stability of Graphene/Ultrathin Bi2Sr2CaCu2O8 Heterostructure under Water Impact. *Int. J. Electrochem. Sci* **2016,** *11*, 738-744.

26. Barns, R. L.; Laudise, R. A., Stability of Superconducting Yba2cu3o7 in the Presence of Water. *Applied Physics Letters* **1987,** *51* (17), 1373-1375.

27. Rosamilia, J. M.; Miller, B.; Schneemeyer, L. F.; Waszczak, J. V.; Obryan, H. M., Aqueous Electrochemistry of Cuprate-Based High-Tc Superconductors. *Journal of the Electrochemical Society* **1987,** *134* (7), 1863-1864.

28. Gogia, B.; Kashyap, S. C.; Pandya, D. K.; Chopra, K. L., Possible Degradation Mechanism of Bscco Superconductors. *Superconductor Science & Technology* **1993,** *6* (7), 497-506.

29. Renner, C.; Revaz, B.; Genoud, J.-Y.; Kadowaki, K.; Fischer, Ø., Pseudogap precursor of the superconducting gap in under-and overdoped Bi 2 Sr 2 CaCu 2 O 8+ δ. *Physical Review Letters* **1998,** *80* (1), 149.

30. Deguire, M. R.; Manas-Zloczower, I.; Tabibazar, M.; Farrell, D. E.; Kim, C. J.; Lu, W. H.; Ng, H.; Rayal, F., Thermosetting Epoxy as a Moisture-Resistant Coating for Yba2cu3o7. *Journal of Materials Science* **1990,** *25* (6), 2881-2885.

31. Novoselov, K. S.; Geim, A. K.; Morozov, S. V.; Jiang, D.; Katsnelson, M. I.; Grigorieva, I. V.; Dubonos, S. V.; Firsov, A. A., Two-dimensional gas of massless Dirac fermions in graphene. *Nature* **2005,** *438* (7065), 197-200.

32. Geim, A. K.; Grigorieva, I. V., Van der Waals heterostructures. *Nature* **2013,** *499* (7459), 419-425.

33. Kresse, G.; Hafner, J., Ab initio molecular dynamics for liquid metals. *Physical review B* **1993,** *47* (1), 558.

34. Perdew, J. P.; Burke, K.; Ernzerhof, M., Generalized gradient approximation made simple. *Physical review letters* **1996,** *77* (18), 3865.

35. Blöchl, P. E., Projector augmented-wave method. *Physical review B* **1994,** *50* (24), 17953.

36. Kresse, G.; Joubert, D., From ultrasoft pseudopotentials to the projector augmented-wave method. *Physical review b* **1999,** *59* (3), 1758.

Supporting Information

Unveil the degradation mechanism of high-temperature superconductor $Bi_2Sr_2CaCu_2O_{8+\delta}$ in water-bearing environments

Yuan Huang[1,2#], Lei Zhang[2,3#], Xiao Cheng Zhou[4#], lei liao[2#], Feng Jin[2], Tao Dong[5], Lin Zhao[2], Yunyun Dai[1], Qiuzhen Cheng[2], Qingming Zhang[2], Li Fen Wang[2], Nan Lin Wang[5], Ming Yue[3], Xuedong Bai[2], Ya Fei Li[4], Qiong Wu[3*], Hong-Jun Gao[2,7], Genda Gu[8], Yeliang Wang[1,6*], Xing-Jiang Zhou[2,7*]

[1]Advanced Research Institute of Multidisciplinary Science, Beijing Institute of Technology, Beijing, 100081, China

[2]Institute of Physics, Chinese Academy of Sciences, Beijing, 100190, China

[3]Faculty of Materials and Manufacturing, Key Laboratory of Advanced Functional Materials, Ministry of Education of China, Beijing University of Technology, Beijing, 100124, China

[4]Jiangsu Key Laboratory of New Power Batteries, Jiangsu Collaborative Innovation Centre of Biomedical Functional Materials, School of Chemistry and Materials Science, Nanjing Normal University, Nanjing, 210023, China

[5]International Center for Quantum Materials, School of Physics, Peking University, Beijing, 100871, China

[6]School of Integrated Circuits and Electronics, MIIT Key Laboratory for Low-Dimensional Quantum Structure and Devices, Beijing Institute of Technology, Beijing, 100081, China

[7]University of Chinese Academy of Sciences, Beijing, 100049, China

[8]Condensed Matter Physics and Materials Science Department, Brookhaven National Lab, Upton, New York, 11973, USA

#These authors contributed equally to this work.
*Correspondence to: wuqiong0506@bjut.edu.cn; yeliang.wang@bit.edu.cn; xjzhou@iphy.ac.cn

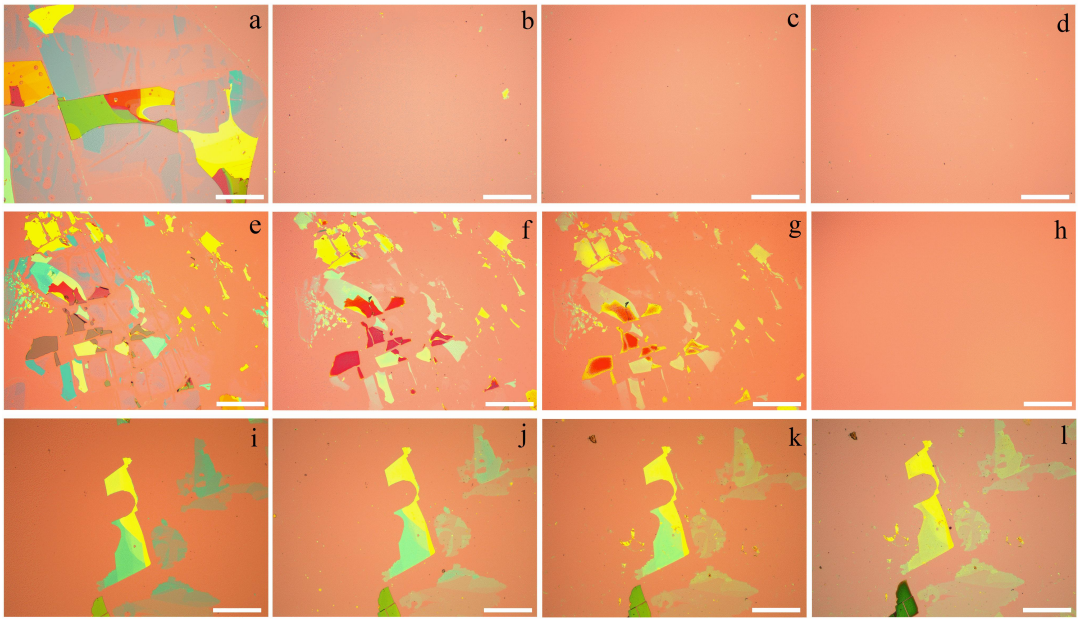

Figure S1. Effects of acid, alkali and salt solutions on exfoliated Bi-2212 flakes. (a-d) Optical micrograph of freshly exfoliated Bi-2212 flakes supported on SiO_2/Si (a) and the same flake after being submerged in acidic solutions for 30 min (b), 1 h (c), 2 h (d). (e-h) Optical micrograph of freshly exfoliated Bi-2212 flakes supported on SiO_2/Si (e) and the same flake after being submerged in alkali solution for 30 min (f), 1 h (g), 2 h (h). (i-l) Optical micrograph of freshly exfoliated Bi-2212 flakes supported on SiO_2/Si (i) and the same flake after being submerged in salt solution for 30 min (j), 1 h (k), 2 h (l). Scale bar：200 μm.

Bi-2212 flakes were exfoliated onto SiO_2/Si substrates, followed by optical microscopy imaging. The substrates were cleaned using acetone, isopropanol and de-ionized (DI) water, and then O_2 plasma was used for further cleaning. After putting PDMS with Bi-2212 flakes in contact with the SiO_2/Si substrate, the substrate was annealed in air at 80 °C for 1 min on a conventional laboratory hot plate. We then cooled down the substrate to room temperature, and finally peeled off the PDMS to complete the exfoliation process. This exfoliation method could improve the yield ratio of the flakes with different thicknesses.

To test the stability of Bi-2212 in acid, alkali and salt solutions, we immersed the exfoliated Bi-2212 flakes in 0.1 mol/L HCl, NaOH and NaCl. After 30 minutes immersion in strong acids, the Bi-2212 flake was completely corroded, as can be seen in Fig. S1 (b). With the extension of immersion time, the thickness of Bi-2212 sheets in alkali solution decrease and are gradually corroded, as can be seen in Fig. S1 (f), (g). After immersion for 2 h, we inspected the flakes again by optical microscopy. But the flakes in NaOH solution disappeared after 2 h (Figure S1 (g)). We assign this to the etching of SiO_2 by NaOH, but not a reaction of NaOH with Bi-2212. Compared with the influence of Bi-2212 in acid and alkali solutions, salt solution has less corrosion effect on Bi-2212. From Fig. S1(i-l), we can see that the thickness of Bi-2212 has become thinner, but the original morphology has not changed.

In addition to discussing the effect of acid-base salt solution on Bi-2212 flakes, we also studied the effect of organic solvents such as acetone and alcohol on Bi-2212 flakes. Figure S2 (a) is optical images of pristine Bi-2212 flakes, captured within 5 min after exfoliation onto a SiO_2/Si substrate. Figure S2 (b) shows the same sample areas after 96 h of exposure to acetone.

At the same time, we also measured the thickness change of Bi-2212 sheet immersed in acetone, as shown in Figure S2 (d-h). The thickness variation diagram is shown in Figure S2 (c). We can see that the thickness of freshly exfoliated Bi-2212 flakes is 90 nm. Even after soaking for 96 hours, the thickness is 84.5 nm, which is only reduced by 5.5 nm, which is completely different from that in acid-base solution. Although the thickness changes little, it can be seen from the AFM image that acetone still has a certain corrosion on the surface of the sample. The surface of the freshly dissociated sample is smooth. After soaking for 96 h, some surfaces become rough and show a sense of particles.

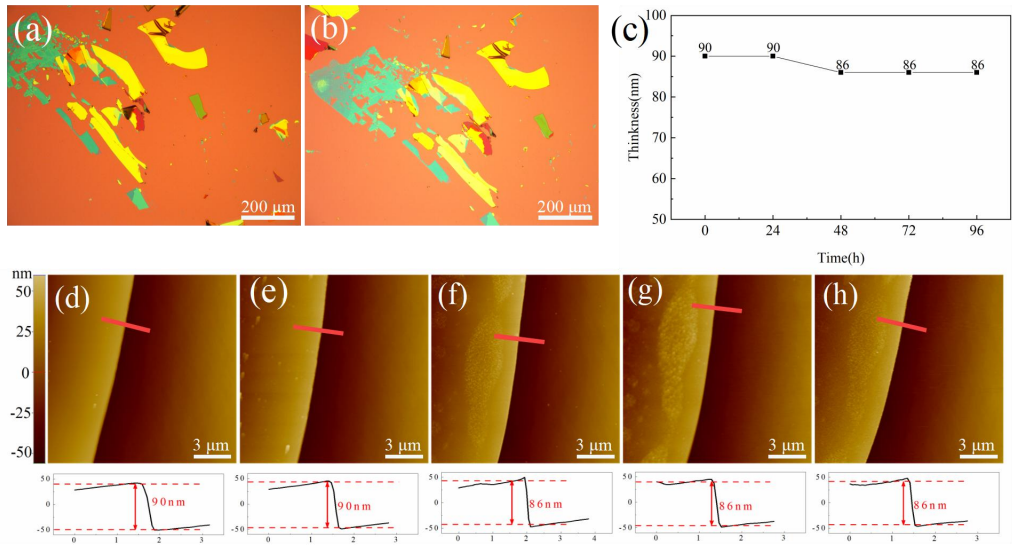

Figure S2. (a) Optical micrograph of freshly exfoliated Bi-2212 flakes supported on SiO_2/Si. (b) Same flakes after being submerged in acetone for 96 h. (c) Variation of Bi-2212 flakes thickness with immersion time in acetone. (d-h) AFM image of a freshly exfoliated Bi-2212 flake (d) and the same flakes after being submerged in acetone for 24 h (e), 48 h (f), 72 h (g), 96 h (h).

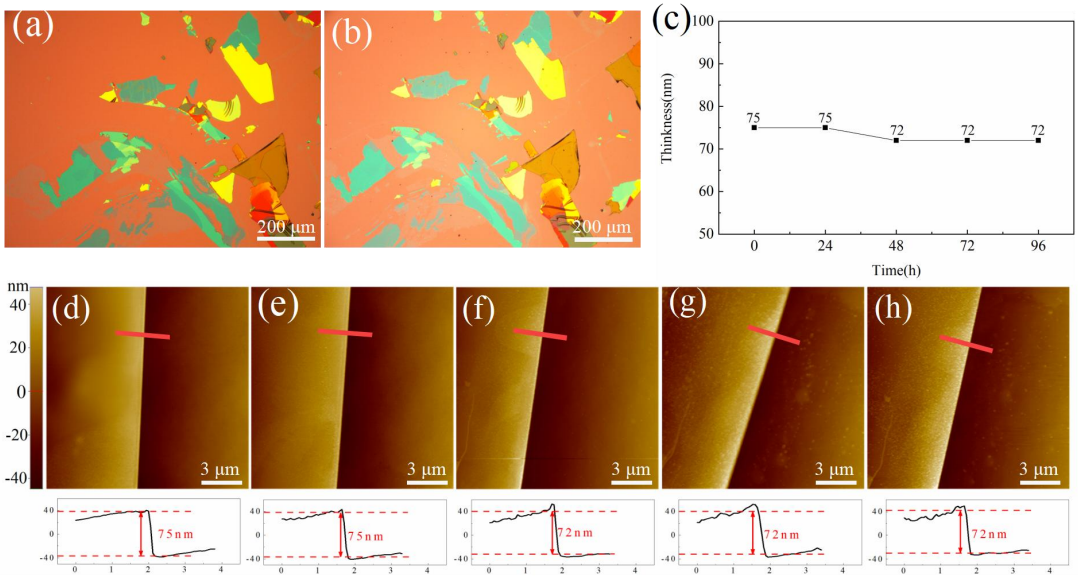

Figure S3. (a) Optical micrograph of freshly exfoliated Bi-2212 flakes supported on SiO_2/Si. (b)

Same flakes after being submerged in ethanol for 96 h. (c) Variation of Bi-2212 flakes thickness with immersion time in ethanol. (d-h) AFM image of a freshly exfoliated Bi-2212 flake (d) and the same flakes after being submerged in ethanol for 24 h (e), 48 h (f), 72 h (g), 96 h (h).

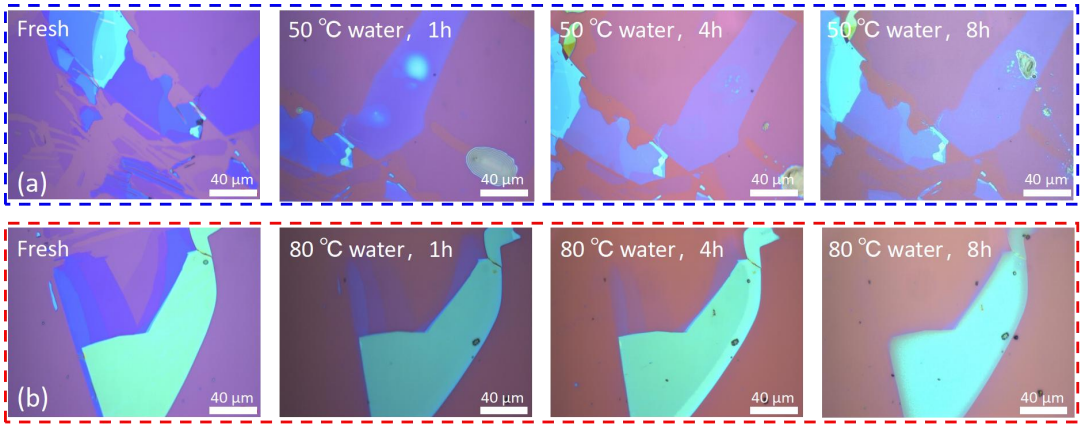

Figure S4. The degradation process of Bi-2212 in hot water. (a) Optical images of one fresh exfoliated Bi-2212 flake and after being immersed in 50 ℃ hot water for 1, 4 and 8 hours. (b) Optical images of another fresh exfoliated Bi-2212 flake and after being immersed in 80 ℃ hot water for 1, 4 and 8 hours. These two sets of comparative data show that the degradation rate of Bi-2212 in hot water is faster than that in water at room temperature.

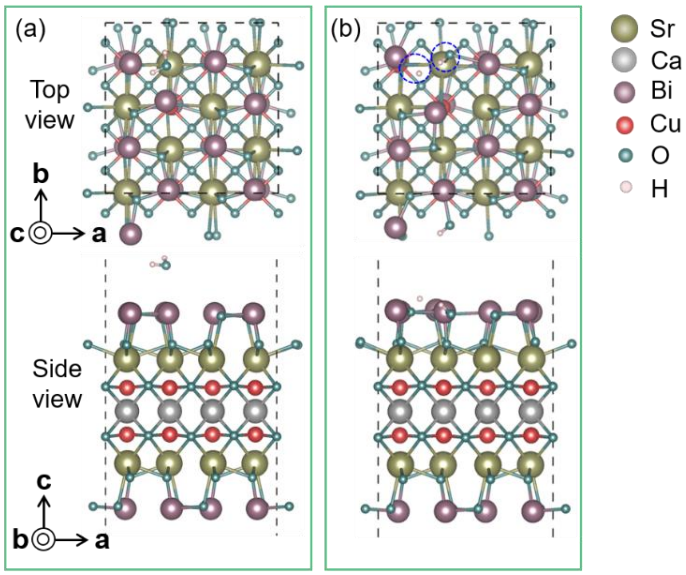

Figure S5. Adsorption and dissociation of H_2O on Bi-2212(001) surface. Atomic structures of (a) physisorbed and (b) chemisorbed H_2O on the surface. The reaction process can be stated as: Bi-2212(001) + H_2O → Bi-2212(OH, H), $\triangle E$ = -0.04 eV.